1064 Center Dr
Gainesville, FL 32611
September 13, 2026

Ms. Orozco Vasquez
University of Florida
1064 Center Drive
Gainesville, FL 32611

Dear Ms. Orozco Vasquez:

The objective of this lab is to quantitate the characteristics of a set of one-meter-long pipes of differing diameter and the elbow associated with the system. This quantitation characterizes the friction factors, head losses, and pipe roughness of the system's pipes, as well as head losses in pipes of 18.94 ± 0.024 mm and 9.42 ± 0.024 mm and the coefficient of loss for the elbow.

Pressure drops and subsequent head losses were evaluated in this experiment to characterize the aforementioned pipe qualities. It is assumed that a fully developed, incompressible, and constant flow was used in pipes of unchanging cross-sectional area and material. The Darcy-Weisbach equations were used for calculating head losses in the pipes due to frictional losses; the Colebrook equation was used for calculating the pipes' friction factors.

A main control valve, in conjunction with an appropriately sized flow meter, was used to control the flow rate in the system while collecting data. Data was collected starting from a flow rate of a nominal 38 ± 1.14 LPM, descending in increments of 10%, with three runs of data collected at each flow rate. Each run set was sampled at 400 samples per second, but the runs differed in the samples per iteration and run time. After a period to ensure fully developed flow for each flow rate, pressure transducers on either side of test sections with inner diameters of 18.94 ± 0.024 mm and 9.42 ± 0.024 mm were used to measure the drop in pressure. This data was recorded using LabVIEW on the lab computer, while data was monitored for egregious recording inaccuracies with the existence of analog gauges on the test setup. Eye protection and close-toed shoes were worn as safety precautions.

The objective to quantify pipe characteristics was met through analysis of the characteristics of the fluid which ran through them. By measuring the characteristics of the flow, frictional forces relating to pipe characteristics could be assessed. For run 3 of the pipe of an inner diameter of 18.94 ± 0.024 mm, which contained the elbow, an initial flowrate of 38.05 ± 1.14 LPM was measured, with a friction factor of 0.0234 ± 0.0014, Reynold's number of 60293 ± 1916, and a head loss of 12.54 ± 0.079 in. The elbow loss coefficient was found to be 1.233 ± 0.074. Finding a roughness factor of 9.52×10^{-4}, the overall pipe roughness of the pipe with the inner diameter 18.94 ± 0.024 mm was found to be $1.72 \times 10^{-5} \pm 2.96 \times 10^{-4}$ m. Uncertainties were calculated through propagation of the Root Sum Squares (RSS) method, and existed as a result of instrumentation inaccuracies including sensitivity, and fluid inconsistencies in density and roughness.

Sincerely,

Erek Dibbern	Gerardo Duran	Yaroslava Izotova	Matthew Sabag
Erek Dibbern	Gerardo Duran	yaroslava Izotova	Matthew Sabag

"On my honor, I have neither given nor received unauthorized aid in doing this assignment."

Table 1: This table displays the large pipe data set, eleven flow settings from thirty-eight LPM down in 10% increments averaged over a five-second window. The nominal flow rate (Q_{nom}) is the targeted setting, and the actual flow rate (Q) is the flowmeter mean, with flowrate uncertainty taken as three percent of that meter's full scale. Head loss is the mean pressure drop converted into inches of water, and the standard deviation represents the scatter within that run. The total uncertainty of head loss (h_L) is found through a root sum of squares, or RSS, which combines the transducer bias with the precision term in quadrature, so neither is counted twice. Temperature is the mean water temperature, and its uncertainty is the thermocouple limit of error which is the tolerance of Type J ($\pm 2.2°C$). As seen from this table, a 10x increase in flow produced only a 24x rise in head loss, not the 100x a constant friction factor predicts, demonstrating that friction factor decreased as Reynolds number increased. This table and all others do not include the data for 0% flow rate as it proved to be unstable. For this data set, 2 samples/iteration at a sampling rate of 400 samples per second for 5 seconds were used.

***Large* pipe Nominal flowrate (LPM)**	**Actual flow rate (LPM)**	**Flowrate uncertainty (± LPM)**	**Head loss Δh (inches)**	**Standard deviation of head loss (inches)**	**Total uncertainty of head loss (± inches)**	**Temperature (°C)**	**Uncertainty in temperature (°C) (std dev + instrument error)**
38	38.22	1.146	13.091	0.1060	0.079	35.99	2.21
34.2	34.24	1.027	10.009	0.0038	0.078	36.3	2.21
30.4	30.49	0.915	8.043	0.0051	0.077	36.43	2.21
26.6	26.53	0.796	6.457	0.0032	0.077	36.7	2.21
22.8	22.73	0.682	5.056	0.0034	0.077	36.94	2.21
19	19.03	0.571	3.903	0.0032	0.076	37.11	2.21
15.2	15.24	0.457	2.798	0.0036	0.076	37.2	2.21
11.4	11.39	0.342	1.912	0.0053	0.076	37.31	2.21
7.6	7.58	0.227	0.736	0.0061	0.076	37.18	2.21
3.8	3.74	0.112	0.537	0.0043	0.076	37.16	2.21

Table 2: Table 2 displays the same eleven large pipe settings recorded with far less averaging, reported every 0.005 seconds across a window of only 0.545 seconds. The headers carry the same meaning as before. The nominal flowrate is the targeted setting, the actual flow rate is the flowmeter mean, and the flowrate uncertainty is three percent of that meter's full scale. Head loss is the mean pressure drop in inches of water and the standard deviation is the scatter of the samples. The total uncertainty of head loss is again a root sum of squares, or RSS, which adds the fixed transducer bias and the random precision term in quadrature rather than directly. Temperature and its uncertainty follow the thermocouple. As seen from Table 2, the shortened window proved costly. The standard deviation ranges from 3.0 to 11.0 inches against 0.089 to 0.216 inches in run 1, and at the three lowest settings the uncertainty exceeds the head loss.

***Large* pipe Nominal flowrate (LPM)**	**Actual flow rate (LPM)**	**Flowrate uncertainty (± LPM)**	**Head loss Δh (inches)**	**Standard deviation of head loss (inches)**	**Total uncertainty of head loss (± inches)**	**Temperature (°C)**	**Uncertainty in temperature (°C) (std dev + instrument error)**
38	38.10	1.143	12.326	0.108	0.079	36.06	2.22
34.2	34.25	1.027	9.754	0.304	0.078	36.35	2.20
30.4	30.49	0.915	7.170	0.275	0.077	36.48	2.22
26.6	26.50	0.795	6.029	0.242	0.077	36.7	2.22
22.8	22.69	0.681	4.367	0.231	0.076	36.94	2.21
19	19.01	0.570	4.851	0.209	0.077	37.12	2.21
15.2	15.28	0.458	2.263	0.249	0.076	37.26	2.21
11.4	11.44	0.343	1.546	0.239	0.076	37.35	2.21
7.6	7.58	0.227	0.708	0.364	0.076	37.26	2.21
3.8	3.75	0.113	0.320	0.357	0.076	37.16	2.21

Table 3: Table 3 displays the large pipe measured with the longest averaging window of the three, reported every 0.5 seconds across 9.5 seconds for twenty samples per setting. The nominal flowrate is the targeted setting, and the actual flow rate is the flowmeter mean, with flowrate uncertainty taken as three percent of that meter's full scale. Head loss is the mean pressure drop in inches of water, and the standard deviation is the scatter within the run. The total uncertainty of head loss comes from a root sum of squares, or RSS, in which the fixed transducer bias and the random precision term are squared, summed, and rooted so that neither dominates unfairly. Temperature is the mean water temperature, and its uncertainty is the thermocouple limit of error. As seen from Table 3, this run proved the most consistent. The scatter never exceeds 0.222 inches, and between 11.4 and 34.2 LPM the head loss matches run 1 within two percent.

***Large* pipe Nominal flowrate (LPM)**	**Actual flow rate (LPM)**	**Flowrate uncertainty (± LPM)**	**Head loss Δh (inches)**	**Standard deviation of head loss (inches)**	**Total uncertainty of head loss (± inches)**	**Temperature (°C)**	**Uncertainty in temperature (°C) (std dev + instrument error)**
38.0	38.05	1.142	12.543	0.090	0.079	36.11	2.22
34.2	34.29	1.029	9.984	0.134	0.078	36.41	2.20
30.4	30.49	0.915	8.055	0.119	0.077	36.48	2.22
26.6	26.49	0.795	6.420	0.100	0.077	36.72	2.22
22.8	22.74	0.682	5.062	0.083	0.077	36.95	2.21
19	18.97	0.569	3.893	0.078	0.076	37.15	2.21
15.2	15.23	0.457	2.853	0.072	0.076	37.26	2.21
11.4	11.44	0.343	1.916	0.116	0.076	37.36	2.21
7.6	7.55	0.226	0.647	0.112	0.076	37.3	2.21
3.8	3.75	0.112	0.430	0.222	0.076	37.16	2.21

Table 4: Table 4 displays a small pipe data set, eleven settings from 34 LPM down to nearly zero across a ten second window. The nominal flowrate is the targeted setting, and the actual flow rate is the flowmeter mean, with flowrate uncertainty taken as three percent of that meter's full scale. Head loss is the mean pressure drop in inches of water, and the standard deviation is the scatter within the run. The total uncertainty of head loss is a root sum of squares, or RSS, which combines the fixed transducer bias with the random precision term in quadrature so that the systematic and random contributions are not simply added. Temperature is the mean water temperature, and its uncertainty is the thermocouple limit of error. As seen from Table 4, the smaller bore produced staggering losses. At 34.079 LPM the small pipe lost 256.144 inches against only 12.543 inches in the large pipe, roughly twenty times more.

Elbow Nominal flowrate (LPM)	Actual flow rate (LPM)	Flowrate uncertainty (± LPM)	Head loss Δh (inches)	Standard deviation of head loss (inches)	Total uncertainty of head loss (± inches)	Temperature (°C)	Uncertainty in temperature (°C) (std dev + instrument error)
34	34.08	1.022	256.144	0.362	0.443	38.19	2.22
30	30.24	0.907	205.827	0.229	0.359	38.27	2.22
27.2	27.20	0.816	170.369	0.227	0.300	38.29	2.22
23.8	23.91	0.717	135.715	0.134	0.244	38.32	2.21
20.4	20.36	0.611	103.259	0.148	0.192	38.39	2.22
17	17.21	0.516	77.667	0.128	0.153	38.42	2.23
13.6	13.65	0.409	51.952	0.086	0.117	38.48	2.22
10.3	10.40	0.312	31.800	0.079	0.093	38.48	2.22
6.8	6.72	0.202	4.619	0.089	0.077	38.31	2.20
3.4	3.40	0.102	0.581	0.099	0.076	38.31	2.20

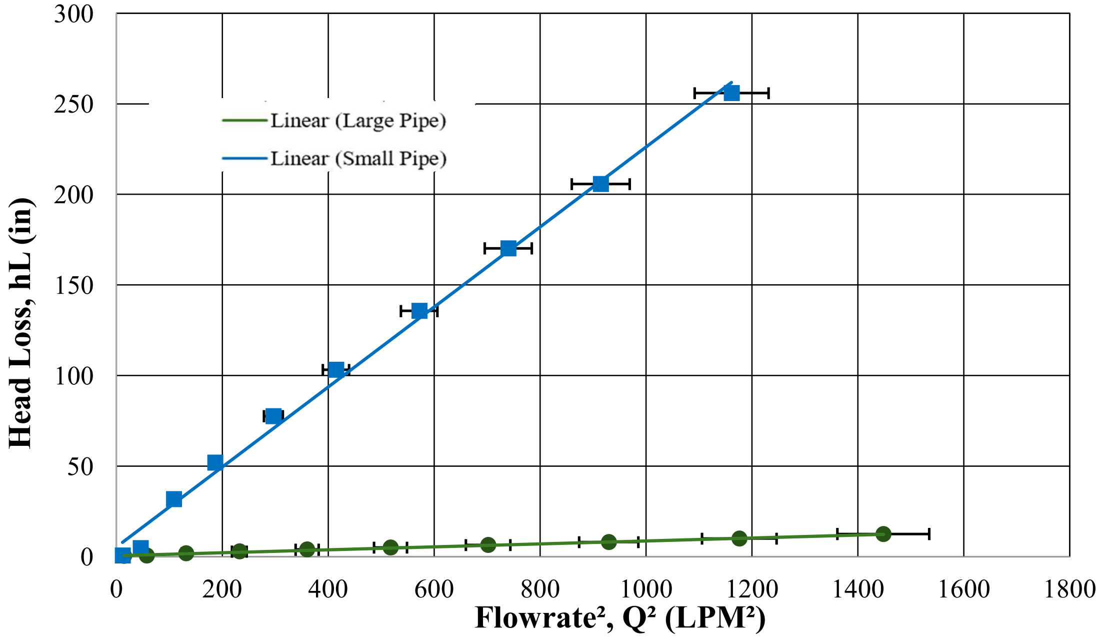

Figure 1: The head loss vs. flowrate² squared data plotted in the figure came from averaging each run's raw pressure and flow readings. Each data point represents a single data cycle, where the flow rate data was first collected at the maximum flowrate, then in successive 10% decrements from that maximum. This 10% decrease was constant at each step, rather than compounding exponentially. At each of the ten flowrates, the transducer's readings of differential pressure were averaged over the run and converted to an equivalent head loss in inches of water. The flow meter's readings were averaged and squared to get flowrate². This was done separately for the large pipe, using the run 3 data, and the small pipe, using its single run, giving ten data points per pipe that were plotted together with propagated uncertainty bars in both directions. The resulting graph shows a direct correlation between head loss and flowrate squared for both pipes. Both series follow the linear trend predicted by the Darcy-Weisbach relationship, confirming that head loss scales with the square of flowrate regardless of pipe size [12]. The small pipe's trendline is far steeper than the large pipes. At the maximum flowrate, the small pipe's cross-sectional area forces the fluid to a higher velocity, and since frictional losses scale with the square of velocity, even a modest flowrate produces disproportionately large head loss. At maximum flowrate, the large and small pipe head losses were 12.5 ± 0.08 in and 256.1 ± 0.44 in respectively roughly a twentyfold difference. The flowrate² uncertainty bars are visible at this scale, while the head loss uncertainty for both pipes is small enough relative to the measured values that it does not noticeable on the scatter plot.

The uncertainty in flowrate squared, Q^2, was found by carrying the flowrate uncertainty through the relationship below, using standard error propagation. Taking the derivative of flowrate squared with respect to flowrate gives the equation below, which simplifies the propagated uncertainty to:

$$U_{Q^2} = \sqrt{(\frac{\partial Q^2}{\partial Q} U_Q)^2} = 2Q \times U_Q = 2 \times 38.05 \times 1.16 = \pm 86.9\ LPM^2$$

For the 100% flowrate point for the large pipe at run 3, this gives an uncertainty of $\pm$ 86.9 LPM². The same calculation was repeated for each of the ten flowrates for large pipe and small pipe to generate the flowrate squared uncertainties.

The following equation was used to calculate the head loss, h_L:

$$h_L = \frac{\Delta P}{\rho g}\ Eqn. 8.25, p. 309, Kundu$$

In this equation, ΔP is the differential pressure, ρ is the density of water, and g is the gravitational constant. An example of a head loss calculation is shown below. The following differential pressure was taken from run 3 100% flow rate.

$$h_L = \frac{0.4518 \frac{\cancel{lb}}{\cancel{in^2}} \times 12^3 \frac{\cancel{in^2} \cdot in}{\cancel{ft^3}}}{\frac{997 \frac{\cancel{kg}}{\cancel{m^3}}}{515.379 \frac{\cancel{kg/m^3}}{\cancel{slug/ft^3}}} \times 32.174 \frac{\cancel{ft}}{\cancel{s^2}}} = 12.54\ in$$

Once all of the variables were converted into same units, head loss of 12.54 in was found. Uncertainty calculations for the previously calculated head loss is shown below:

$$U_{h_L} = \sqrt{\left(\frac{\partial h_L}{\partial \Delta P} U_{\Delta P}\right)^2 + \left(\frac{\partial h_L}{\partial \rho} U_\rho\right)^2 + \left(\frac{\partial h_L}{\partial g} U_g\right)^2}$$

This equation uses the RSS (Root Sum of Squares) method to combines uncertainty from three sources, pressure, density, and gravity [13]. For each variable, it multiplies how sensitive head loss is to that variable the partial derivative by that variable's own uncertainty. RSS then combines these three contributions by squaring each one, adding them together, and taking the square root, since simply adding them directly would overestimate the total uncertainty.

Below are the examples of solved partial derivatives:

$$\frac{\partial h_L}{\partial \Delta P} = \frac{1}{\rho g} = \frac{1}{0.0361 \frac{lb}{in^2 \cdot \cancel{in}} \times 386.089 \frac{\cancel{in}}{s^2}} = 0.0717 \frac{in^2 \cdot s^2}{lb}$$

$$\frac{\partial h_L}{\partial \rho} = -\frac{\Delta P}{\rho^2 g} = -\frac{0.4518\ \frac{lb}{in^2}}{0.0361^2\ \frac{\mathrm{lb}\cdot \cancel{\mathrm{lb}}}{in^5 \cdot \cancel{in}} \times 386.089 \frac{\cancel{in}}{s^2}} = -\ 0.898\ \frac{in^3 \cdot s^2}{lb}$$

$$\frac{\partial h_L}{\partial g} = -\frac{\Delta P}{\rho g^2} = -\ \frac{0.4518\ \frac{\cancel{lb}}{\cancel{in^2}}}{0.0361\ \frac{\cancel{lb}}{\cancel{in^2} \cdot in} \times \left(386.089\ \frac{\cancel{in}}{s^2}\right)^2} = -\ 0.0000836\ \frac{s^4}{in}$$

Final solved equation for 12.54 in uncertainty head loss becomes:

$U_{h_L} = \sqrt{(0.0717 \times 1.061)^2 + (-0.898 \times 0.023)^2 + (-0.0000836 \times 0.001)^2} = \pm\ 0.0790$ in

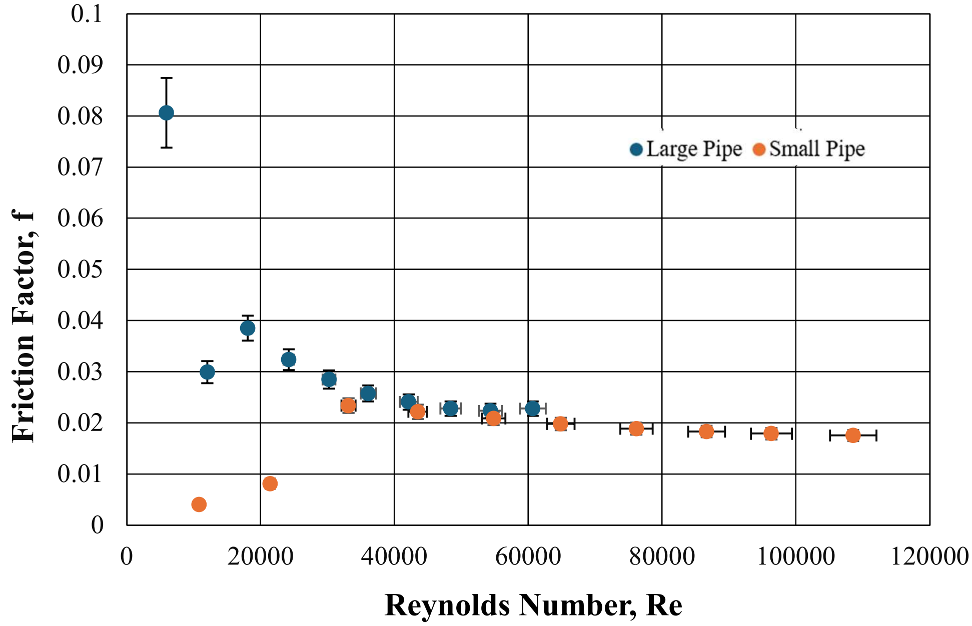

Figure 2: In the graph above, friction factors versus Reynolds number for the large pipe and small pipe are shown, with uncertainty bars in both quantities. Both series follow the expected Moody-plot trend of decreasing friction factor with increasing Reynolds number, converging toward a similar value at the highest Reynolds numbers tested. However, there's an outlier in the data. The small pipe's lowest Reynolds point of 10816 ± 3448 has a friction factor of only 0.004 ± 0.0011, below the trend the rest of the series follows. This is consistent with low flow measurement noise in the differential pressure reading. At low flow rates, the pressure drops across the pipe is small, so the transducer's fixed noise becomes a much larger fraction of the measured value. The same noise that's negligible at high flow can affect the reading substantially at low flow. Since head loss is calculated directly from this pressure reading, and friction factor is in calculated from head loss, that noise propagates through the calculation and can pull the computed friction factor off the expected trend.

To calculate the friction factor, equation below was used, where D is the diameter of the pipe.

$$f = \frac{gh_L}{8L}\left(\frac{\pi D^{\frac{5}{2}}}{Q}\right)^2 \;\; Eqn.8.26, p.309, Kundu$$

The RSS Equation for the friction factor of uncertainty is:

$$U_f = \sqrt{\left(\frac{\partial f}{\partial L}\cdot U_L\right)^2 + \left(\frac{\partial f}{\partial g}\cdot U_g\right)^2 + \left(\frac{\partial f}{\partial h_L}\cdot U_{h_L}\right)^2 + \left(\frac{\partial f}{\partial \pi}\cdot U_\pi\right)^2 + \left(\frac{\partial f}{\partial D}\cdot U_D\right)^2 + \left(\frac{\partial f}{\partial Q}\cdot U_Q\right)^2}$$

$$U_f = \sqrt{\begin{matrix}\left(-\frac{h_L\cdot D^5\cdot \pi^2\cdot g}{8\cdot L^2\cdot Q^2}\cdot U_L\right)^2 + \left(\frac{h_L\cdot D^5\cdot \pi^2}{8\cdot L\cdot Q^2}\cdot U_g\right)^2 + \left(\frac{D^5\cdot \pi^2\cdot g}{8\cdot L\cdot Q^2}\cdot U_{h_L}\right)^2 \\ + \left(\frac{2\cdot h_L\cdot D^5\cdot \pi\cdot g}{8\cdot L\cdot Q^2}\cdot U_\pi\right)^2 + \left(\frac{5\cdot h_L\cdot D^4\cdot \pi^2\cdot g}{8\cdot L\cdot Q^2}\cdot U_D\right)^2 + \left(-\frac{2\cdot h_L\cdot D^5\cdot \pi^2 g}{8\cdot L\cdot Q^3}\cdot U_Q\right)^2\end{matrix}}$$

With the partials substituted, the units cancel as so:

$$\frac{\partial f}{\partial L} = -\frac{h_L\cdot D^5\cdot \pi^2\cdot g}{8\cdot L^2\cdot Q^2}$$

$$= -\frac{12.5427\ \cancel{in}\cdot(0.7441)^5\ \cancel{in^5}\cdot\pi^2\cdot 386.088\frac{\cancel{in}}{\cancel{s^2}}}{8\cdot(39.3701)^2\ in^{\cancel{2}}\cdot(1.01706)^2\frac{\frac{\cancel{in^6}}{\cancel{s^2}}}{\cancel{LPM^2}}\cdot(38.05)^2\ \cancel{LPM^2}} = -0.0005871\ in^{-1}$$

$$\frac{\partial f}{\partial g} = \frac{h_L\cdot D^5\cdot \pi^2}{8\cdot L\cdot Q^2} = \frac{12.5427\ \cancel{in}\cdot(0.7441)^5\ \cancel{in^5}\cdot\pi^2}{8\cdot 39.3701\ in\cdot(38.7018)^2\ \cancel{in^6}/s^2} = 0.00005986\ s^2\cdot in^{-1}$$

$$\frac{\partial f}{\partial h_L} = \frac{D^5\cdot \pi^2\cdot g}{8\cdot L\cdot Q^2} = \frac{(0.7441)^5\ \cancel{in^5}\cdot\pi^2\cdot 386.088\frac{\cancel{in}}{\cancel{s^2}}}{8\cdot 39.3701\ in\cdot(38.7018)^2\ \cancel{in^6/s^2}} = 0.001843\ in^{-1}$$

$$\frac{\partial f}{\partial \pi} = \frac{2\cdot h_L\cdot D^5\cdot \pi\cdot g}{8\cdot L\cdot Q^2} = \frac{2\cdot 12.5427\ \cancel{in}\ \cdot(0.7441)^5\ \cancel{in^5}\cdot\pi\cdot 386.088\frac{\cancel{in}}{\cancel{s^2}}}{8\cdot 39.3701\ \cancel{in}\cdot(38.7018)^2\ \cancel{in^6/s^2}} = 0.01471$$

$$\frac{\partial f}{\partial D} = \frac{5\cdot h_L\cdot D^4\cdot \pi^2\cdot g}{8\cdot L\cdot Q^2} = \frac{5\cdot 12.5427\ \cancel{in}\cdot(0.7441)^4\ \cancel{in^4}\cdot\pi^2\cdot 386.088\frac{\cancel{in}}{\cancel{s^2}}}{8\cdot 39.3701\ in\cdot(38.7018)^2\ \cancel{in^6/s^2}} = 0.1553\ in^{-1}$$

$$\frac{\partial f}{\partial Q} = -\frac{2\cdot h_L\cdot D^5\cdot \pi^2 g}{8\cdot L\cdot Q^3}$$

$$= \frac{2\cdot 12.5427\ \cancel{in}\ \cdot(0.7441)^5\ \cancel{in^5}\cdot\pi^2\cdot 386.088\frac{\cancel{in}}{\cancel{s^2}}}{8\cdot 39.3701\ \cancel{in}\cdot(38.7018)^3\frac{\cancel{in^6}\cdot in^3}{s^{\cancel{3}}}} = 0.001194\ s\cdot in^{-3}$$

The flowmeter uncertainty of 3% was provided in the report description [1]. Raw flowrate data was averaged from each cycle's data and multiplied by 0.03 to calculate the uncertainty values.

$$U_L = 0\ in$$

$$U_g = 0.196850394\ in \cdot s^{-2}$$

$$U_{h_L} = 0.079049623\ in$$

$$U_\pi = 0.001$$

$$U_D = 0.000745669\ in$$

$$U_Q = 1.161054846\ in^3 \cdot s^{-1}$$

$$U_f = \sqrt{\begin{array}{c}(-0.0005871\ in^{-1} \cdot 0\ in)^2 + (0.00005986\ s^2 \cdot in^{-1} \cdot 0.196850394\ in \cdot s^{-2})^2 \\ +(0.001843\ in^{-1} \cdot 0.079049623\ in)^2 + (0.01471 \cdot 0.001)^2 \\ +(0.1553\ in^{-1} \cdot 0.000745669\ in)^2 + (0.001194\ s \cdot in^{-3} \cdot 1.161054846\ in^3 \cdot s^{-1})^2\end{array}}$$

$$U_f = \pm\, 0.001407054$$

Reynold's equation used is shown below:

$$Re_D = \frac{\rho \cdot V \cdot D}{\mu}\ Eqn.\,1.27, p.\,13, Kundu$$

Where V is the flow velocity, and μ viscosity of water. The RSS equation used to determine the uncertainty in the Renold's number is:

$$U_{Re_D} = \sqrt{\left(\frac{\partial Re_D}{\partial \rho} \cdot U_\rho\right)^2 + \left(\frac{\partial Re_D}{\partial V} \cdot U_V\right)^2 + \left(\frac{\partial Re_D}{\partial D} \cdot U_D\right)^2 + \left(\frac{\partial Re_D}{\partial \mu} \cdot U_\mu\right)^2}$$

$$U_{Re_D} = \sqrt{\left(\frac{V \cdot D}{\mu} \cdot U_\rho\right)^2 + \left(\frac{\rho \cdot D}{\mu} \cdot U_V\right)^2 + \left(\frac{\rho \cdot V}{\mu} \cdot U_D\right)^2 + \left(-\frac{\rho \cdot V \cdot D}{\mu^2} \cdot U_\mu\right)^2}$$

With the partials substituted, the units cancel as so:

$$\frac{\partial Re_D}{\partial \rho} = \frac{V \cdot D}{\mu} = \frac{2.2510\ m/\cancel{s} \cdot 0.01894\ m}{0.000705\ kg/m \cdot \cancel{s}} = 60.4737\ m^3 \cdot kg^{-1}$$

$$\frac{\partial Re_D}{\partial V} = \frac{\rho \cdot D}{\mu} = \frac{997\ \cancel{kg}/m^{\cancel{3}} \cdot 0.01894\ \cancel{m}}{0.000705\ \cancel{kg}/\cancel{m} \cdot s} = 26784.6525\ s \cdot m^{-1}$$

$$\frac{\partial Re_D}{\partial D} = \frac{\rho \cdot V}{\mu} = \frac{997\ \cancel{kg}/m^{\cancel{3}} \cdot 2.2510\ \cancel{m}/\cancel{s}}{0.000705\ \cancel{kg}/\cancel{m} \cdot \cancel{s}} = 318329.1\ m^{-1}$$

$$\frac{\partial Re_D}{\partial \mu} = -\frac{\rho \cdot V \cdot D}{\mu^2} = \frac{997\,\frac{kg}{m^3} \cdot 2.2510\,\frac{m}{s} \cdot 0.01894\,m}{(0.000705)^2\,\frac{kg^2}{m^2} \cdot s^2} = 85520925.9\; m \cdot s/kg$$

$$U_\rho = 0.21\; kg/m^3$$

$$U_V = 0.0677\; m/s$$

$$U_D = 0.05\; m$$

$$U_\mu = 7.05 \times 10^{-6}\; kg/m \cdot s$$

With all the partial derivatives found, an example for Reynold's number uncertainty calculation for the large pipe, run 3 is shown as:

$$U_{Re_D} = \sqrt{\begin{array}{c} \left(60.4737\; m^3 \cdot kg^{-1} \cdot 0.21\,\frac{kg}{m^3}\right)^2 + (26784.6525\; s \cdot m^{-1} \cdot 0.0677\; m/s)^2 \\ +(26784.6525\; s \cdot m^{-1} \cdot 0.05\; m)^2 + \left(85520925.9\; m \cdot \frac{s}{kg} \cdot 7.05 \times 10^{-6}\,\frac{kg}{m} \cdot s\right)^2 \end{array}}$$

$$U_{Re_D} = \pm 1916.9855$$

In order to find velocity of water, the following equation was used:

$$V = \frac{Q}{A} = \frac{4Q}{\pi D^2}\; Eqn.\, 8.21, p.\, 308, Kundu$$

The RSS uncertainty of velocity of water becomes:

$$U_V = \sqrt{\left(\frac{\partial V}{\partial Q} \cdot U_Q\right)^2 + \left(\frac{\partial V}{\partial D} \cdot U_D\right)^2}$$

$$U_V = \sqrt{\left(\frac{4}{\pi \cdot D^2} \cdot U_Q\right)^2 + \left(-\frac{8 \cdot Q}{\pi \cdot D^3} \cdot U_D\right)^2}$$

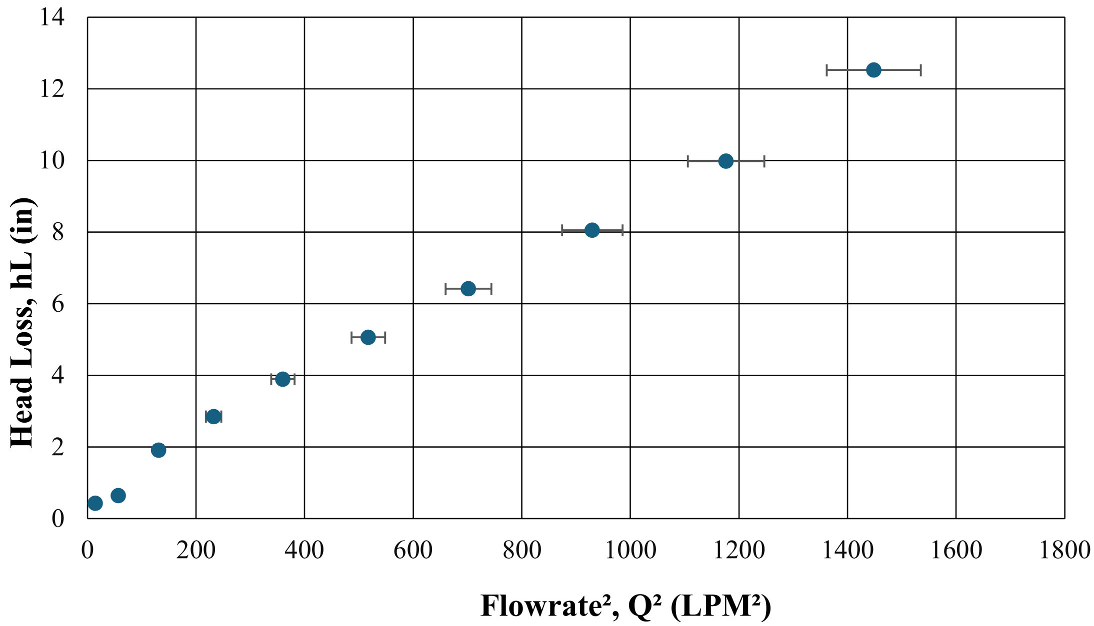

Figure 3: Run 3 data was used to create this plot. The flow rate was measured with a Proteus ball valve that has a 3% accuracy rating. This linear relationship between the flow rate and head loss is reflected in a slope which determines the loss coefficient. The elbow configuration is the joint of the large pipe configuration. The uncertainty of head loss has a magnitude that is not able to be seen withing the plot since the magnitude is low.

The graph in Figure 3 presented head loss versus flow rate squared utilized the head loss:

$$h_L = K_L \frac{V^2}{2gc} \quad Eqn. 8.25, p. 309, Kundu$$

Is rearranged into:

$$K_L = \frac{2h_L g}{V^2}$$

Provided as a sample calculation for the loss coefficient, from run 3 of the large pipe:

$$K_L = \frac{2(12.54\ in)(386.088\ \frac{in}{s^2})}{(88.623\frac{in}{s})^2} = 1.233$$

$$U_{K_L} = \sqrt{\left(\frac{\partial K_L}{\partial h_L} U_{h_L}\right)^2 + \left(\frac{\partial K_L}{\partial g} U_g\right)^2 + \left(\frac{\partial K_L}{\partial V} U_V\right)^2}$$

$$\frac{\partial K_L}{\partial h_L} = \frac{2g}{V^2}, \qquad \frac{\partial K_L}{\partial g} = \frac{2h_L}{V^2}, \qquad \frac{\partial K_L}{\partial V} = -\frac{4h_L g}{V^3}$$

Provided as a sample calculation for the uncertainty loss coefficient, from run 3 of the large pipe:

$$\frac{\partial K_L}{\partial h_L} = \frac{2(386.08\ \frac{\cancel{in}}{\cancel{s^2}})}{(88.62\ \frac{in}{s})^{\cancel{2}}} = 0.098\ in^{-1}, \qquad \frac{\partial K_L}{\partial g} = \frac{2(12.54\ \cancel{in})}{88.62^2\ \frac{in^{\cancel{2}}}{s^2}} = 0.003\ s^2 \cdot in^{-1},$$

$$\frac{\partial K_L}{\partial V} = -\frac{4(12.54\ \cancel{in})(386.09\ \frac{\cancel{in}}{\cancel{s^2}})}{88.62^3\ \frac{in^{\cancel{3}}}{s^{\cancel{3}}}} = -0.028\ s \cdot in^{-1}$$

The complete uncertainty sample calculation can be represented as:

$$U_{K_L} = \sqrt{((0.098)(0.079))^2 + ((0.003)(0.19685))^2 + \left((-0.028)(0.60)\right)^2} = \pm\ 0.0185$$

Table 5: The table summarizes the loss coefficient, K_L , for the 90° elbow at each of the ten flowrates, calculated from the large pipe's un 3 data using the equations shown previously, along with the propagated uncertainty in K_L.

Flow Rate (%)	**Actual Flow Rate (LPM)**	**Head Loss, h_L**	**Loss Coefficient, K_L**	**Uncertainty in K_L (±)**
100%	38.05	12.543	1.233	0.0746
90%	34.29	9.984	1.209	0.0673
80%	30.49	8.055	1.234	0.0599
70%	26.49	6.420	1.303	0.0522
60%	22.74	5.062	1.393	0.0450
50%	18.97	3.893	1.540	0.0377
40%	15.23	2.853	1.750	0.0306
30%	11.44	1.916	2.082	0.0235
20%	7.54	0.647	1.617	0.0165
10%	3.75	0.430	4.359	0.0746

The Colebrook equation, Reynold's number, & the friction factors result in a roughness factor equation [1]. The roughness factor equation reflects the relative roughness that reflects how flow resistance is influenced by surface irregularities.

$$\frac{1}{\sqrt{f}} = -2log\left(\frac{\frac{\epsilon}{D}}{3.7} + \frac{2.51}{Re\sqrt{f}}\right)$$

Given a Reynolds number and friction factor, the Colebrook equation can be transformed to solve for the relative roughness.

$$\frac{\epsilon}{D} = 3.7\left(10^{-\frac{1}{2\sqrt{f}}} - \frac{2.51}{Re\sqrt{f}}\right)$$

Using run 3 of the Large Pipe the 100% case was calculated:

$$\frac{\epsilon}{D} = 3.7\left(10^{-\frac{1}{2\sqrt{0.0233}}} - \frac{2.51}{60293\sqrt{0.0233}}\right) = 9.52 \times 10^{-4}\ m$$

Multiplying the roughness factor by the diameter of the pipe the relative roughness can be determined

$$\left(\frac{\epsilon}{D}\right) \cdot D = 1.72 \times 10^{-5}\ m$$

This roughness can then be compared to the property of a copper pipe 0.003mm [2]. This difference

The RSS equation for uncertainty of the roughness factor is:

$$U_{\frac{\epsilon}{D}} = \sqrt{\left(\frac{\partial \frac{\epsilon}{D}}{\partial f} U_f\right)^2 + \left(\frac{\partial \frac{\epsilon}{D}}{\partial Re} U_{Re}\right)^2}$$

$$\frac{\partial \frac{\epsilon}{D}}{\partial Re} = \frac{9.287}{60293^2\sqrt{0.0233}} = 1.70 \times 10^{-8}$$

$$U_{\frac{\epsilon}{D}} = \sqrt{((0.2098)(0.0014))^2 + ((1.70 \times 10^{-8})(1916))^2} = \pm\, 2.96 \times 10^{-4}$$

Table 6: The variables are presented with their respective coefficients, values, uncertainty, and unit of measure. Standard deviation & a 95% confidence interval were used to determine the inner pipe diameter uncertainty. Manufacturer specifications informed uncertainty for pressure, flow rate, & temperature [9-11]. Pipe length uncertainty was determined by performing an uncertainty analysis.

Variable	**Coefficient**	**Value**	**Uncertainty**	**Unit**
Inner Diameter Small Pipe	I.D.S.	18.94	$\pm$ 0.011	mm
Inner Diameter Large Pipe	I.D.L.	9.42	$\pm$ 0.021	mm
Pressure	P	1014	$\pm$ 4	mbar
Flow Rate	Q	Varies	$\pm$ 0.03	LPM
Temperature	T	20.6	$\pm$ 0.04	Celsius
Pipe Length	L	1000	$\pm$ 0.05	mm

To determine the entrance length of the pipe diameter (D) and Reynolds number (R_e) are used. This region marks the start of the pipe to the beginning of the fully developed region in the pipe. Performed for turbulent flow regions where the Reynolds number exceeds 4000, the equation presented below calculates the length in mm [13]. The datapoints at 0% flowrate were neglected as the Reynold number is 0 in those cases, which distorts the calculation.

$$L_e = 4.4D(R_e)^{\frac{1}{6}}\,Eqn.\,12.65, p.\,511, Kundu$$

Table 7: Entrance lengths ensure the movement of the fluid through the system is allowed to develop appropriately. In the case of the full flow rate in the large pipe, the entrance length is about half of the length of the pipe which marks a well-designed system. For the large pipe, run 3 was selected to ensure the largest dataset was analyzed. The entrance length was calculated for both the large and small pipe diameters in the turbulent region. As nominal flow rates decreased in each pipe diameter, the entrance diameter decreased. The principle of entrance length in fluid mechanics builds the theory that faster developing boundary layers result in shorter entrance length as lower flow rates correspond to lower Reynolds numbers.

Nominal Flow Rate (LPM)	Pipe Diameter (mm)	Entrance Length (mm)	Flow Type
38.05	18.93	521.848	Turbulent
34.29	18.93	512.878	Turbulent
30.49	18.93	502.926	Turbulent
26.49	18.93	491.274	Turbulent
22.74	18.93	478.949	Turbulent
18.97	18.93	464.689	Turbulent
15.23	18.93	448.006	Turbulent
11.44	18.93	427.149	Turbulent
7.54	18.93	398.493	Turbulent
3.75	18.93	354.637	Turbulent
34.08	9.42	286.277	Turbulent
30.24	9.42	280.631	Turbulent
27.20	9.42	275.717	Turbulent
23.90	9.42	269.849	Turbulent
20.36	9.42	262.717	Turbulent
17.21	9.42	255.460	Turbulent
13.65	9.42	245.784	Turbulent
10.40	9.42	234.886	Turbulent
6.72	9.42	218.424	Turbulent
3.40	9.42	194.917	Turbulent

This report explored the differences between three runs of the large diameter pipe. During the first run, 2 samples/iteration with a sample rate of 400 samples per second and a run time of 5 seconds were used. For the second run, 200 samples/iteration with a sampling rate of 400 samples per second and a run time of 5 seconds. For the third run, the 200 samples/iteration with a sampling rate of 400 samples per second and a run time of 10 seconds.

For this report, the sample rate did not change with a value of 400 Hz. Samples per iteration and runtime were the two variables. Since run 3 was performed with the highest of run time and samples per iteration, it was considered the most accurate. This was reflected in the low uncertainty values and low standard deviations within the data. The sample procedure reflects a data chunk size and frequency change Since this was the longest runtime and the highest sampling rate then it averaged over a larger sample size and therefore represented the true readings more accurately.

To calculate the loss coefficient, the flow coefficient (C_v) and diameter (D) in equation [] were used. The valve type determines the characteristics of the flow, size, and the shape which influences the loss coefficient through this equation.

$$\frac{890D^4}{(C_v)^2}$$

Table 8: This table represents the valve types that are numbered, labeled with what type of valve type, photo, loss coefficient, and reference. Valves 3 and 6 are from the pipe fitting table that provided friction loss. Referencing the equation and manufacturer data, the loss coefficients were calculated for all other valves

Number	Valve Type	Photo	Loss Coefficient	Reference
1	Ball Check		7.3636	[3]
2	Butterfly		1.035	[4]
3	Ball		0.05	[6]
4	Three Way		3.94675	[7]

5	Piston Spring Check		13.8	[4]
6	Globe		10	[5]
7	Gate		0.15	[5]
8	Needle		96.4119	[6]
9	Flow-Teck Ball		1.96	[8]

References

[1] "New Pipe Loss Lab 25-1. pdf", University of Florida, EML4147, Canvas.

[2] "Surface Roughness Coefficients" https://www.engineeringtoolbox.com/surface-roughness-ventilation-ducts-d_209.html#gsc.tab=0 (accessed September 13, 2026).

[3] "TC Series True Union Ball Check Valves", https://valveman.com/content/hayward-tc-series-specification-sheet-valveman.com.pdf (accessed September 13, 2026).

[4] "Pipe Fitting K-Factor Table (Crane TP-410)", https://simupipe.com/resources/k-factor-table (accessed September 13, 2026).

[5] "Pipe Flows – Head Losses", https://engineering.purdue.edu/~wassgren/teaching/ME30800/NotesAndReading/PipeFlows_Losses_LectureNotes.pdf (accessed September 13, 2026).

[6] "Noshok Products", https://catalog.noshok.com/products/504-mfc (accessed September 13, 2026).

[7] "Rubinetterie Brescaine", https://www.ultravalve.co.uk/wp-content/uploads/2019/12/brass-valves-and-regulators-5210.pdf (accessed September 13, 2026).

[8] "FLOTECH Your Valve and Automation Experts", https://www.flotechinc.com/ball/ (accessed September 13, 2026).

[9] "HIGH ACCURACY PRESSURE TRANSDUCERS", https://assets.omega.com/pdf/test-and-measurement-equipment/pressure/pressure-transducers/PX409_Series.pdf (accessed September 13, 2026).

[10] "200 Series Flow Meters", https://www.proteusind.com/wp-content/uploads/2016/06/200DS.pdf (accessed September 13, 2026).

[11] "Fisherbrand™ Traceable™ Digital Barometer", https://www.fishersci.com/shop/products/traceable-digital-barometer/S25098#?keyword=s25098 (accessed September 13, 2026).

[12] "Darcy-Weisbach Equation: Flow Resistance & Pressure Loss Calculator", The Engineering ToolBox, https://www.engineeringtoolbox.com/darcy-weisbach-equation-d_646.html#gsc.tab=0 (accessed September 13, 2026)

[13] "Fluid Mechanics", P. K. Kundu, I. M. Cohen, and D. R. Dowling, 7th ed. San Diego, CA: Academic Press, 2022, Ch. 8 & 12. doi.org (accessed September 13, 2026).

Name	**Date**	**Hours Worked**	**Description of Tasks Performed**
Slava	9/7/26	3	Working on data organization, and data calculations
Slava	9/8/26	6	Data validation, made the excel sheets to calculate data, plots
Slava	9/13/26	5	Formatting, equation calculations
Gerardo	9/7/26	3	Looking at run 3 data and making uncertainty equations excels
Gerardo	9/8/26	6	Processed data and created plots
Gerardo	9/13/26	5	Developed tables and found structure for the sample calculations
Matthew	9/7/26	3	Organizing files, creating teams, categorizing file types, delegating work.
Matthew	9/8/26	6	Developing the partials for the uncertainties
Matthew	9/13/26	5	Processing data and organizing tables
Erek	9/7/26	3	Reynolds and friction factor hand calculations.
Erek	9/8/26	6	Excel formatting and developing error
Erek	9/13/26	5	Roughness and loss coefficient calculations and preparing letter
	Total Hours:	**56**	